Published in Geochimica et Cosmochimica Acta 66/23 : 4069-4083, 2002,
which should be used for any reference to this work

Dysaerobic conditions during Heinrich events 4 and 5: Evidence from phosphorus distribution in a North Atlantic deep-sea core

FEDERICA TAMBURINI,[1,*] SYLVAIN HUON,[2] PHILIPP STEINMANN,[1] FRANCIS E. GROUSSET,[3] THIERRY ADATTE,[1] and KARL B. FÖLLMI[1]

[1]Institut de Géologie, Université de Neuchâtel, Case Postale 2, Rue Emile Argand 11, 2007 Neuchâtel, Switzerland
[2]UMR 7618 Biogéochimie Isotopique, Université Pierre et Marie Curie, Case Postale 120, Place Jussieu 4, 75252 Paris cedex 05, France
[3]UMR 5805 EPOC, Département de Géologie et Océanographie, Université Bordeaux I, Avenue des Facultés, 33405 Talence cedex, France

Abstract—Reactive phosphorus undergoes diagenetic transformation once transferred into marine sediments. The degree of regeneration and redistribution of phosphorus depends on early diagenetic and environmental conditions, which may be linked to larger scale phenomena, such as bottom water circulation, water column ventilation, and organic carbon flux. Phosphorus phases of the <50-μm-sized fraction of deep-sea sediments from core SU 90-09 (North Atlantic, 43°31'N, 30°24'W, 3375 m below sea level) have been analyzed using a sequential extraction technique (SEDEX method) to reconstruct phosphorus geochemistry during Heinrich events 4 and 5. Comparison with Holocene samples from the same site indicates that postdeposition diagenetic transformation has not affected phosphorus distribution in the deep part of the sediments. Total and reactive phosphorus average 0.40 ± 0.04 mg/g and 0.30 ± 0.05 mg/g, respectively, and are comparable to values found in analog deep-sea environments in the North Atlantic. Detrital phosphorus, the phase linked to igneous- and metamorphic-derived material, sharply increases during Heinrich events and covaries with the ice-rafted debris record, whereas authigenic and Fe-bound phosphorus phases, both influenced by redox conditions, decrease or even disappear. These findings suggest that during the deposition of Heinrich layers (HLs), environmental parameters hampered the precipitation of these phases. Large freshwater discharges in relation to iceberg surges may have provoked a temporary stratification of the water column. Accordingly, dysaerobic conditions in the sediments may have fostered the loss of dissolved phosphorus from the sediments to the water column, in a direct and rapid response to the changed conditions. Decreasing trends in organic matter elemental ratios (total organic carbon/organic phosphorus) and Rock-Eval oxygen index values, along with the presence of partly authigenic dolomite and ankerite within HLs, also support this assumption.

1. INTRODUCTION

During the last glaciation (marine isotope stages 2 to 4), six episodes of enhanced ice-rafted debris (IRD) supply produced the so-called Heinrich layers (HLs) (Heinrich, 1988; Broecker et al., 1992; Andrews, 1998). These layers, found across the North Atlantic down to 40°N in the area called IRD belt (Ruddiman, 1977), contrast sharply with ambient glacial sedimentation. They are characterized by the sequential deposition of high amounts of lithogenic material, which originated from both European and Canadian soil and rock sources (Grousset et al., 2000), high detrital carbonate contents (Bond et al., 1992), low amounts of foraminiferal tests (Heinrich, 1988; Broecker et al., 1992), and a high supply of organic matter derived from terrestrial sources (e.g., Rosell-Melé et al., 1997; Huon et al., 2002). There is convincing evidence that HL deposition was accompanied by the formation of a freshwater lid (Bond et al., 1992), which possibly stopped or strongly reduced North Atlantic deep water (NADW) formation and thermohaline circulation (Broecker, 1994; Paillard and Labeyrie, 1994; Maslin et al., 1995; Vidal et al., 1997; Zahn et al., 1997). The signature of Heinrich events has been found not only in North Atlantic sediments (e.g., the Arabian and South China seas; Schulz et al., 1998; Wang et al., 1999) but also in terrestrial records (e.g., Grimm et al., 1993; Lowell et al., 1995; Benson et al., 1996; Sanchez-Goñi et al., 2000) and has been correlated with the Greenland ice core isotope record (Bond et al., 1993), pointing to possible teleconnections between high- and low-latitude climates on short time scales.

The present study addresses the geochemical signature of Heinrich events 4 and 5, as expressed in their marine phosphorus records. Phosphorus is an essential nutrient, limiting oceanic productivity on geological time scale (Tyrrell, 1999). Being involved in biologic processes and having a strong affinity to iron and manganese oxyhydroxides, the P cycle in marine sediments is rather complex and controlled by environmental conditions (for a comprehensive review, see Jarvis et al., 1994; Krajewski et al., 1994; Föllmi, 1996; Delaney, 1998). Regenerated dissolved and reactive (i.e., biologically available) P is potentially redistributed to different sedimentary phases or rediffused into the water column, depending on chemical and physical parameters, such as phosphorus and fluoride concentrations in pore waters, dissolved oxygen levels, alkalinity, nature of sediments, and bioirrigation (Krajewski et al., 1994; Van Cappellen and Ingall, 1994; Slomp, 1997; Colman and Holland, 2000). Being influenced by parameters that may change quite rapidly, P phase concentrations in sediments are expected to fluctuate at a comparable rate.

In that sense, constraints on the redistribution and recycling of P during the deposition of HLs are consequential because phosphate concentrations in bottom waters, inferred from

* Author to whom correspondence should be addressed (ftamburini@whoi.edu).

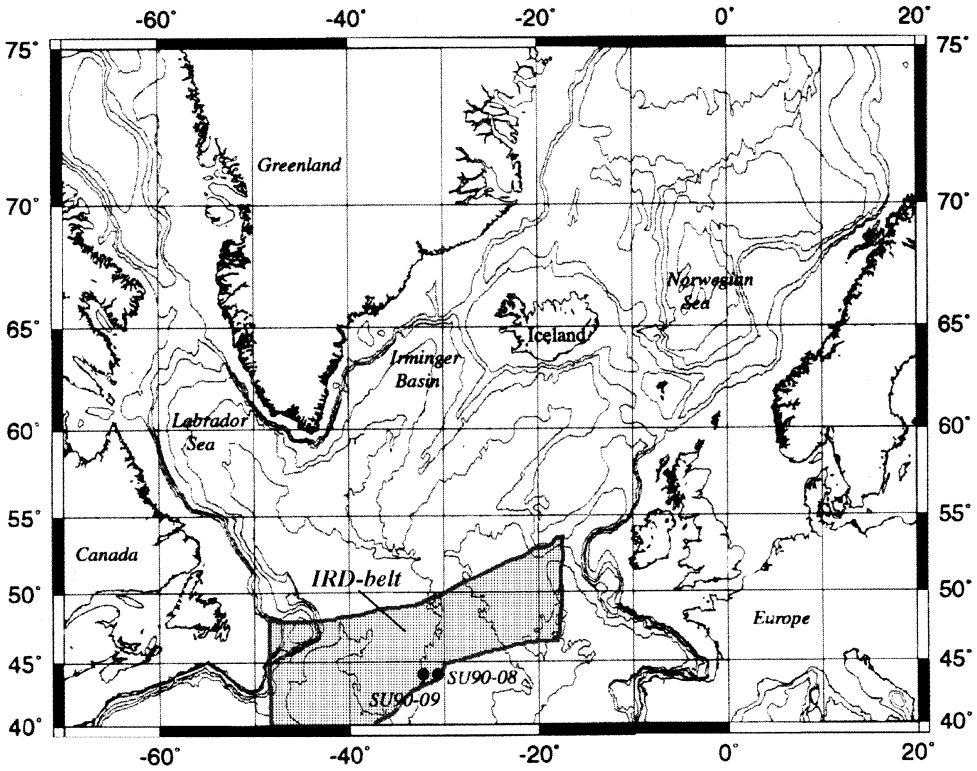

Fig. 1. Location of core SU90-09 in the central North Atlantic. The map was obtained through the Aquarius Geomar Online Map Creation (http://www.aquarius.geomar.de/omc). The gray area represents the "Ruddiman ice-rafted debris (IRD) belt" (Ruddiman, 1977).

Cd/Ca and $\delta^{13}C$ measurements on benthic foraminifers, are widely used to assess changes in oceanic circulation related to these rapid climatic changes. Because cadmium and phosphate profiles in the water column show a high similarity, cadmium is considered a "phosphate analog" in deep-sea paleoceanographic studies (Boyle, 1988). The increase in the Cd/Ca ratio of benthic foraminifers recorded during HL deposition (Bertram et al., 1995; Marchal et al., 1999) has been interpreted as the result of the reduction or even shutoff of NADW formation and the consequent northward penetration of nutrient- and phosphate-rich waters from the South Atlantic Ocean.

It is therefore important to determine the extent of recycling of dissolved phosphorus from sediments and its contribution to the total phosphate concentration in bottom waters during Heinrich events. We believe that a clear understanding of P geochemistry in the marine environment during and between Heinrich events may contribute to a better interpretation of the bottom water environment (oxic and suboxic conditions), water column dynamics, and circulation. The aim of this study is to provide a high-resolution record of fine-sized (<50 μm) P compounds in marine sediments from a North Atlantic deep-sea core (including HLs 4 and 5), using a sequential P extraction procedure to (a) estimate the contribution of detrital P during the phases of enhanced ice-rafting detritus supply; (b) determine the influence of this supply on reactive P redistribution in sediments; and (c) discuss some of the factors controlling bottom water conditions during Heinrich events using P sedimentary cycling as a proxy for oxic vs. anoxic conditions.

2. MATERIAL AND METHODS

Sediment samples were recovered from piston core SU90-09 (43°05'N, 31°05'W, 3375 m below sea level), located in the central North Atlantic on the western side of the Mid-Atlantic Ridge (Fig. 1; Grousset et al., 2001; Huon et al., 2002). Stratigraphic correlation with reference core SU90-08 (43°31'N, 30°24'W) and the down-core position of HLs 1 to 5 were performed using accelerator mass spectrometry ^{14}C ages on *Neogloboquadrina pachyderma s.* shells, coarse lithic grain (>150 μm) counts under binocular, low-field magnetic susceptibility, and gray-scale reflectance records (methods described in Grousset et al., 1993; Cortijo et al., 1995; Grousset et al., 2001).

Our study focuses on the fine-sized (<50 μm) fraction of 83 samples recovered within and between HLs 4 and 5. Samples were taken from 130- to 200-cm core depths at 1-cm interval between HLs and at 0.5 cm within HLs 4 and 5, which were identified at core depths of 144.0 to 153.5 cm and 187.0 to 193.5 cm, respectively (Huon et al., 2002). Thirteen samples between 10 and 30 cm, representing Holocene (postglacial) sediments, were also analyzed to better constrain the possible overprint of diagenesis on P. The use of the <50-μm-sized fraction of sediments for this study is justified by four main reasons: (a) Organic matter from the <50-μm fraction from the same samples was analyzed for nitrogen and carbon stable isotopes (Huon et al., 2002), so it is possible to compare results from both studies; (b) terrigenous organic matter (and related organic-bound P), transported "far off" its continental source, is rather concentrated in the fine-sized fraction, either dispersed in the sediment or bound to clay minerals (Keil et al., 1994; Christensen, 1996); (c) in continental source areas, organic matter is stabilized in the fine-sized fraction of soils (Balesdent and Mariotti, 1996), and therefore, a better characterization of continental inputs is expected from fine-sized fractions; and (d) the ratio of organic carbon vs. lithic content of bulk sediment is very low, particularly for HLs, which are enriched in coarse IRD, leading to high mineral matrix effects and reducing as much the resolution of elemental analysis.

Table 1. Scheme of the phosphorus sequential extraction technique (SEDEX, modified after Ruttenberg, 1992).

Step name	Treatments	P component isolated[a]	Errors[b]	Detection limits[c]
Iron-bound P[d]	10 mL CBD solution (6 hr) (0.22 mol/L sodium citrate, 0.11 mol/L sodium bicarbonate, 0.13 mol/L sodium dithionite), 10 mL 1 mol/L $MgCl_2$ (2 hr), 10 mL H_2O (2 hr)	Exchangeable or loosely sorbed P, reducible or reactive iron-bound P plus ferric Fe	3 to 6%	0.001
Authigenic P[e]	10 mL 1mol/L Na-acetate buffered to pH 4 with acetic acid (5 hr), 10 mL 1mol/L $MgCl_2$ (2 hr), 10 mL 1mol/L $MgCl_2$ (2 hr), 10 mL H_2O (2 hr)	Carbonate fluorapatite, biogenic hydroxyapatite	2 to 7%	0.025
Detrital P[e]	10 mL 1N HCl (16 hr)	Detrital fluorapatite-bound P	3 to 5%	0.003
Organic P[e]	1 mL 50% (w/v) $MgNO_3$, dry in low oven, ash at 500°C (2 hr), 10 mL 1 N HCl (24 hr)	Organic-bound P	2 to 5%	0.004

[a] Concentrations of all phases are expressed in milligrams per gram of sediment.
[b] Errors for each phase determination are considered as the relative standard deviation calculated on replicate analyses of consistency standards.
[c] Detection limits are considered as 3 times relative standard deviation calculated on replicate analyses of blank solutions.
[d] Iron-bound phosphorus and ferric Fe concentrations were measured using inductively coupled plasma atomic emission spectroscopy.
[e] The other phases were measured using a spectrophotometer. Sample solutions were diluted in distilled water, and a color developping agent was added to the solution, following the ascorbic acid method for phosphate (Eaton et al 1995).

Moreover, it has been shown that fine-sized fractions in deep-sea sediments of the NE Atlantic provide unambiguous records of enhanced ice rafting detrital supply. Drastic changes in mineralogical composition and K-Ar apparent ages support a high contribution of continental derived material for even finer sized fractions, such as clay-sized (<2 μm) fractions (Bond et al., 1992; Huon and Ruch, 1992; Jantschik and Huon, 1992; Huon and Jantschik, 1993; Broecker, 1994).

Phosphorus was extracted from the <50-μm-sized fraction of the sediment samples using the SEDEX method, a sequential extraction technique (Ruttenberg, 1992; Filippelli and Delaney, 1996; Anderson and Delaney, 2000). Fe-bound, authigenic, detrital, and organic-bound P represent the four extracted P phases that are linked to different sedimentary sinks (see Table 1 for details, errors, and detection limits of the method). Fe- and organic-bound P correspond to P linked to Fe and Mn oxyhydroxides and to organic matter, respectively. The acetate step of the SEDEX method (step 2; see Table 1) extracts phosphorus associated with authigenic fluorapatite, fish debris, calcium carbonate, and smectite (Ruttenberg, 1992). In all cases, as dissolved P is removed either from the water column or from the sediments, we can consider and refer to it as authigenic. Ferric Fe from both amorphous and well-crystallized minerals and Fe from amorphous Fe sulfides have been extracted during the first step of the SEDEX method (for details on the methodology, see Table 1 and Slomp et al., 1996).

One concern about studying the <50-μm fraction is the possibility of losing information about P phase concentrations. Therefore, we have also performed phosphorus extractions on bulk sediments from selected HL and ambient glacial samples. Fe-bound P and organic-bound P concentrations in both bulk and fine-sized fraction are in the same range of values, confirming the assumptions that (a) P associated with Fe oxyhydroxides is mainly present in the fine fraction (Slomp et al., 1996), and (b) organic matter is mainly concentrated in this fraction (see discussion above). Detrital P concentrations are slightly higher in bulk sediments than in the <50-μm fraction, but being nonreactive, detrital P is not affected by postburial redistribution. Moreover, considering its covariance with the IRD record (see below), detrital P in the fine fraction still records detrital supply changes. Authigenic P is the phase more affected by grain size, and bulk sediments bear larger amounts of authigenic P (approximatively twice as much). This implies that we possibly underestimate a part of the authigenic P that precipitates on larger particles. Nevertheless, the differences in concentration between bulk sediments and the <50-μm fraction are consistent, and we are confident in using the results from the fine-sized fraction to support the interpretation of changing environmental conditions in the sediments.

The approximate values of organic-bound hydrogen (in terms of hydrogen index [HI], mg HC/g total organic carbon [TOC]) and organic-bound oxygen (in terms of oxygen index [OI], mg CO_2/g sediment) were obtained from Rock-Eval pyrolysis (Espitalié et al., 1986). Because our samples are rich in carbonate minerals (i.e., calcite and dolomite) and have very low TOC contents (<0.5%), the measured values could be potentially biased. The reason is that some of the CO_2 produced from carbonate decomposition during pyrolysis at relatively low temperature overlaps with the CO_2 originating from organic matter. In our samples, this phenomenon leads to a systematic overestimation of OI and to an underestimation of TOC and HI. We evaluated these effects by analyzing a subset of decarbonated (1 mol/L HCl) samples, which were selected both from ambient glacial and HL sediments. The OI and HI values calculated before and after carbonate removal are well and linearly correlated (r^2 = 0.946 and 0.785 for OI and HI, respectively), and the carbonate-free samples reveal the same trends as the untreated samples (i.e., higher HI and lower OI within HLs compared to ambient glacial sediments). We have therefore corrected the values obtained for bulk samples using the linear correlations of OI and HI in carbonate-free vs. untreated samples. Even though this correction may not remove all uncertainty on the absolute values, the relative trends are reliable and allow us to compare them with other organic matter proxies, such as $\delta^{13}C$, obtained on carbonate-free <50-μm-sized fractions of the same samples (Huon et al., 2002).

Bulk sediment mineralogy was determined by X-ray diffraction (XRD) (2θ CuKα, Scintag XDS 2000 diffractometer) using a semi-quantitative estimation based on external standards (Kübler, 1987). Calcite, dolomite, and ankerite form a solid solution in which Ca^{2+} may be replaced by Fe^{3+} and/or Mg^{2+}. Dolomite and ankerite have overlapping d spacings, and it is commonly difficult to distinguish between them. Therefore, we have separated the major (104) peaks of these two minerals at around 31° 2θ CuKα using a peak profile Pearson VI deconvolution function (Scintag, 1987; Kübler et al., 1990). The relative error on mineralogical percentages is ~5%.

3. RESULTS

The down-core variations in the concentrations of different P phases within the fine-grained fraction for the Holocene and glacial sediments are displayed in Figures 2 and 3, together with low-field magnetic susceptibility values (Grousset et al., 2001), IRD content, fine-sized TOC concentrations, and $\delta^{13}C$ values (Huon et al., 2002). According to the magnetic susceptibility and IRD records (Fig. 3), HL 4 is characterized by a rather broad peak shape, whereas HL 5 is narrower (Grousset et al., 2001). The distribution of IRD in the sediment is not limited to the interval defined by foraminifer minima and IRD maxima (Heinrich, 1988; Bond et al., 1992), but is more widespread

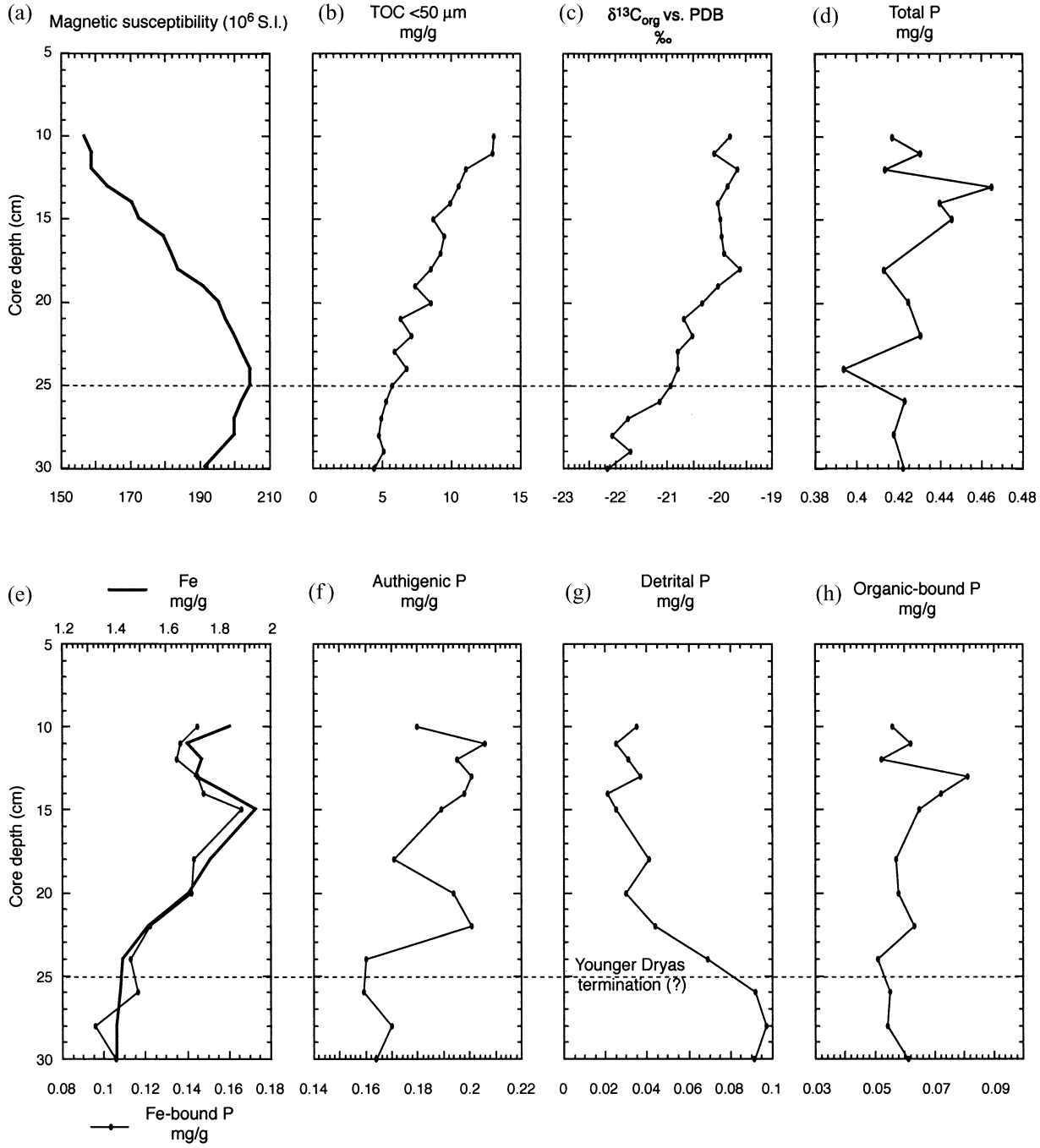

Fig. 2. Plots of down-core variations of (a) magnetic susceptibility (Grousset et al., 2001); (b) total organic carbon (TOC) content and (c) $\delta^{13}C$ of organic carbon of the <50-μm fraction (Huon et al., 2002); (d) total phosphorus; (e) ferric Fe and Fe-bound P; (f) authigenic P; (g) detrital P; and (h) organic-bound P for the fine-sized fraction of Holocene samples from core SU 90-09. The dotted line represents the inferred Younger Drays termination (Huon et al., 2002). PDB = Pee Dee Belemnite standard.

because of the sequential deposition of detrital minerals, closely monitored by magnetic susceptibility values (Fig. 3).

Total P concentrations in Holocene and ambient glacial samples range between 0.33 and 0.46 mg/g (Figs. 2 and 3, Table 2) and are comparable with total P concentrations reported for the low-productivity region in the North Atlantic (<0.5 mg/g; Baturin, 1988; Ruttenberg and Berner, 1993). Fe-bound, authigenic, and organic-bound P concentrations are also comparable with concentrations measured in sediments of the North Atlantic (Ocean Drilling Program Site 907; Tamburini, unpublished data). Concentrations of most P phases in the Holocene samples are in the range of the values observed between 130 and 200 cm for ambient glacial sediments. However, Fe-bound P and reducible Fe concentrations, extracted

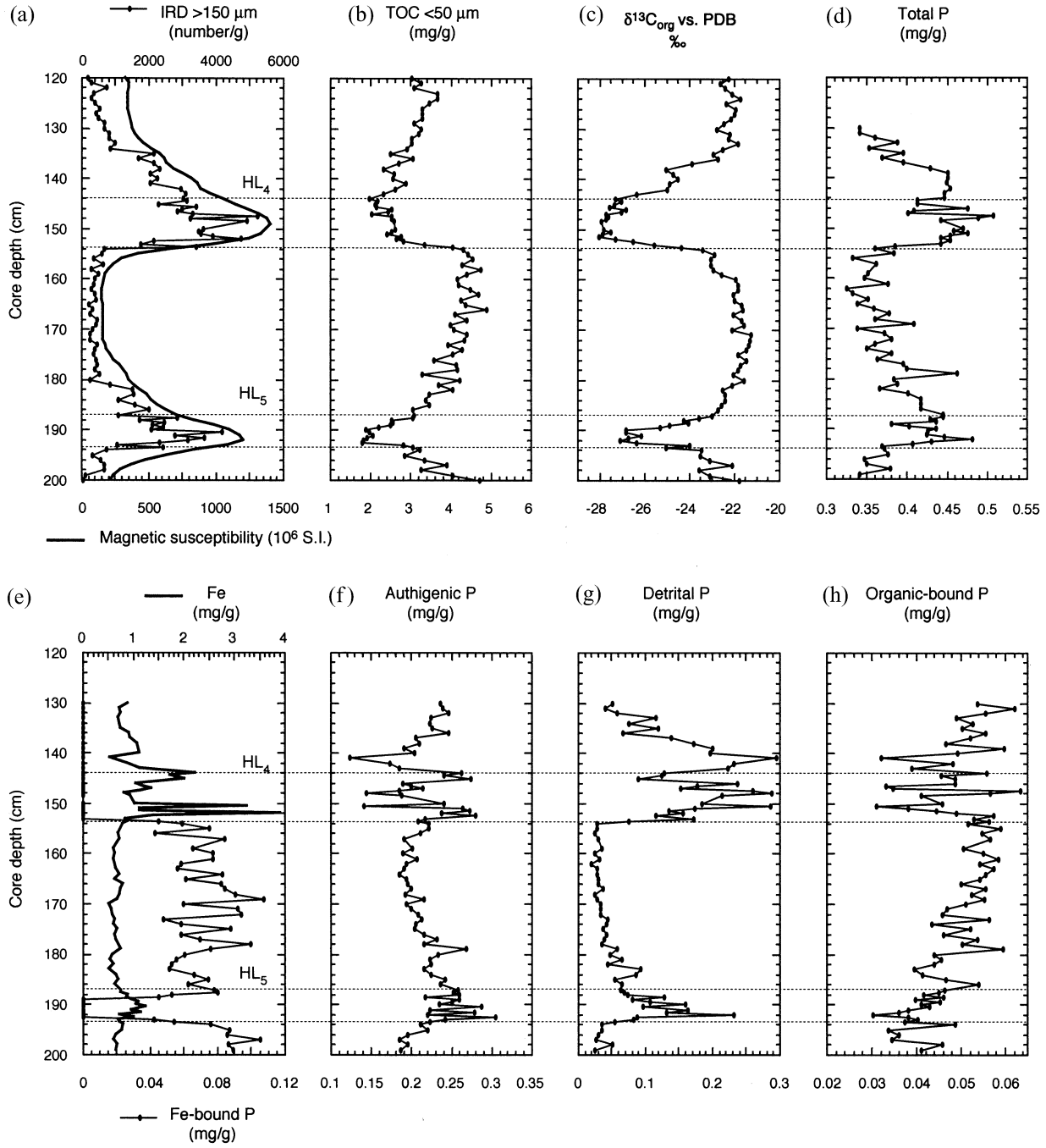

Fig. 3. Plots of down-core variations of (a) magnetic susceptibility and ice-rafted debris (IRD) (>150 μm) content (Grousset et al., 2001); (b) total organic carbon (TOC) content and (c) $\delta^{13}C$ of organic carbon of the <50-μm fraction (Huon et al., 2002); (d) total phosphorus; (e) ferric Fe and Fe-bound P; (f) authigenic P; (g) detrital P; and (h) organic-bound P for the fine-sized fraction of samples from core SU 90-09 (130 to 200 cm depth). The 144.0- to 153.5-cm and 187.0- to 193.5-cm intervals represent the Heinrich events 4 and 5, respectively (Huon et al., 2002). PDB = Pee Dee Belemnite standard, HL = Heinrich layer.

during the first step of the SEDEX method (Ruttenberg, 1992; Slomp et al., 1996), exhibit higher values for Holocene samples than for ambient glacial sediments.

Detrital P concentrations in the Holocene sediments average 0.0320 ± 0.0078 mg/g above 25 cm and increase to 0.094 ± 0.003 mg/g between 25 and 30 cm. This latter depth corresponds to the termination of the Younger Dryas event (Mangerud et al., 1974), although its position in the sedimentary column is only a rough estimation based on fine-sized organic matter TOC and $\delta^{13}C$ records (Fig. 2; see also Huon et al., 2002). In contrast with detrital P, authigenic P, Fe-bound P, and Fe concentrations display concomitant decreasing trends to-

Table 2. Phosphorus phases and iron concentrations of fine-grained sediments from core SU 90-09 (North Atlantic, IRD belt).

Depth (cm)	Sediment type	Fe mgFe/g	Fe-bound P mgP/g	Authigenic P mgP/g	Detrital P mgP/g	Organic-bound P mgP/g	Total P mgP/g
SU 90-09	(Holocene)						
10		1.846	0.145	0.180	0.035	0.056	0.415
11		1.682	0.137	0.206	0.025	0.062	0.430
12		1.739	0.135	0.195	0.031	0.052	0.413
13		1.716	0.145	0.201	0.037	0.081	0.464
14		1.835	0.148	0.198	0.021	0.072	0.439
15		1.943	0.166	0.189	0.025	0.065	0.444
18		1.769	0.143	0.171	0.041	0.057	0.412
20		1.688	0.142	0.194	0.030	0.058	0.424
22		1.534	0.122	0.201	0.044	0.063	0.429
24		1.432	0.113	0.160	0.069	0.051	0.393
26		1.423	0.116	0.159	0.092	0.055	0.423
28		1.410	0.096	0.170	0.097	0.054	0.417
30		1.406	0.106	0.164	0.091	0.061	0.422
SU 90-09							
130		0.894	0.000	0.236	0.051	0.054	0.341
131		0.724	0.000	0.239	0.040	0.062	0.341
132		0.739	0.000	0.246	0.059	0.056	0.360
133		0.706	0.000	0.224	0.115	0.049	0.388
134		0.718	0.000	0.224	0.076	0.053	0.352
135		0.739	0.000	0.226	0.119	0.050	0.395
136		0.908	0.000	0.246	0.067	0.056	0.369
137		0.939	0.000	0.205	0.138	0.052	0.395
138		1.084	0.000	0.209	0.173	0.047	0.428
139		1.105	0.000	0.190	0.201	0.060	0.450
140		1.129	0.000	0.205	0.197	0.049	0.451
141		0.530	0.000	0.123	0.295	0.032	0.450
142		0.881	0.000	0.173	0.232	0.048	0.453
143		1.115	0.000	0.185	0.223	0.039	0.447
144	H4	2.219	0.000	0.263	0.128	0.056	0.447
144.5	H4	1.732	0.000	0.241	0.125	0.046	0.412
145	H4	2.014	0.000	0.274	0.090	0.049	0.413
145.5	H4						
146	H4	1.056	0.000	0.189	0.237	0.049	0.475
146.5	H4	1.166	0.000	0.199	0.176	0.033	0.409
147	H4	1.348	0.000	0.214	0.152	0.035	0.402
147.5	H4	1.144	0.000	0.184	0.259	0.063	0.507
148	H4	0.818	0.000	0.144	0.288	0.057	0.488
148.5	H4	0.944	0.000	0.187	0.213	0.041	0.442
150	H4	1.023	0.000	0.240	0.185	0.046	0.470
150.5	H4	3.248	0.000	0.141	0.286	0.031	0.457
151	H4	1.126	0.000	0.264	0.173	0.038	0.476
151.5	H4	1.123	0.000	0.273	0.135	0.045	0.453
152	H4	3.900	0.000	0.237	0.156	0.049	0.443
152.5	H4	1.404	0.000	0.279	0.116	0.058	0.453
153	H4	0.850	0.000	0.216	0.172	0.053	0.442
153.5	H4	0.892	0.045	0.208	0.075	0.056	0.384
154		0.800	0.059	0.221	0.028	0.052	0.359
155		0.757	0.075	0.222	0.027	0.059	0.384
156		0.691	0.043	0.211	0.025	0.055	0.333
157		0.715	0.084	0.191	0.029	0.057	0.361
158							
159		0.603	0.065	0.200	0.036	0.050	0.352
160		0.643	0.077	0.190	0.025	0.055	0.347
161		0.614	0.077	0.207	0.032	0.058	0.375
162		0.637	0.058	0.194	0.019	0.054	0.325
163		0.651	0.056	0.190	0.028	0.057	0.332
164		0.729	0.083	0.184	0.027	0.056	0.351
165		0.631	0.061	0.193	0.030	0.054	0.338
166		0.803	0.082	0.196	0.030	0.050	0.358
167		0.738	0.084	0.200	0.037	0.055	0.377
168		0.725	0.091	0.192	0.025	0.052	0.360
169		0.677	0.108	0.216	0.029	0.055	0.408
170		0.514	0.059	0.194	0.034	0.051	0.339
171		0.573	0.092	0.199	0.033	0.047	0.371
172		0.596	0.094	0.208	0.033	0.046	0.380
173		0.644	0.047	0.212	0.044	0.056	0.360

(continued)

Table 2. (Continued)

Depth (cm)	Sediment type	FemgFe/g	Fe-bound P mgP/g	Authigenic P mgP/g	Detrital P mgP/g	Organic-bound P (mgP/g)	Total P mgP/g
174		0.604	0.058	0.205	0.042	0.043	0.349
175		0.684	0.088	0.203	0.037	0.052	0.380
176		0.626	0.058	0.216	0.042	0.046	0.362
177		0.666	0.069	0.232	0.039	0.054	0.394
178		0.712	0.100	0.215	0.034	0.050	0.399
179		0.756	0.076	0.269	0.058	0.059	0.462
180		0.587	0.060	0.233	0.047	0.044	0.384
181		0.546	0.055	0.223	0.064	0.046	0.388
182		0.612	0.053	0.225	0.044	0.044	0.365
183		0.520	0.051	0.216	0.093	0.040	0.400
184		0.661	0.066	0.225	0.085	0.041	0.418
185		0.710	0.074	0.241	0.055	0.047	0.417
186		0.631	0.063	0.236	0.065	0.054	0.417
187	H5	0.743	0.078	0.257	0.063	0.046	0.445
187.5	H5	0.748	0.080	0.253	0.068	0.045	0.445
188	H5	0.893	0.053	0.260	0.074	0.042	0.428
188.5	H5	0.856	0.045	0.217	0.127	0.046	0.436
189	H5	0.964	0.000	0.260	0.081	0.040	0.380
189.5	H5	1.102	0.000	0.250	0.107	0.045	0.403
190	H5	1.055	0.000	0.235	0.159	0.041	0.436
190.5	H5	1.239	0.000	0.287	0.097	0.043	0.426
191	H5	0.960	0.000	0.222	0.164	0.038	0.424
191.5	H5	1.158	0.000	0.279	0.131	0.036	0.446
192	H5	0.715	0.000	0.220	0.231	0.030	0.481
192.5	H5	1.000	0.000	0.305	0.088	0.038	0.430
193	H5	0.714	0.042	0.242	0.083	0.040	0.407
193.5	H5	0.724	0.054	0.223	0.055	0.037	0.369
194		0.787	0.076	0.212	0.035	0.049	0.371
195		0.775	0.087	0.219	0.036	0.034	0.376
196		0.666	0.086	0.195	0.030	0.036	0.347
197		0.599	0.105	0.185	0.026	0.034	0.350
198		0.670	0.086	0.196	0.051	0.046	0.378
199		0.651	0.089	0.186	0.025	0.041	0.341

ward the assumed Younger Dryas upper boundary. HLs 4 and 5 are characterized by high concentrations of detrital P, which show a fivefold increase compared to ambient glacial sediment values (Fig. 3). The distribution of detrital P concentrations in HL 4 displays two major peaks of fine-sized detrital P supply. The first one is coeval with the maximum IRD concentration (144 to 153.5 cm, Fig. 3), while the second one (137 to 142 cm, Fig. 3) occurs immediately after HL 4, when the level of IRD supply is still high. The top and bottom of HL 4 bear lower amounts of detrital P. Coarse IRD contents (>150 μm) and fine-sized detrital P (<50 μm) concentrations show similar profiles, but the correlation is not statistically meaningful for HLs ($r^2 = 0.26$, $n = 32$). In HLs 4 and 5, authigenic P is closely linked to detrital P distribution. Detrital and authigenic P phases are roughly correlated in ambient glacial sediments ($r^2 = 0.36$, $n = 44$), whereas a relatively well-defined inverse correlation is observed for HL samples (Fig. 4; $r^2 = 0.65$, $n = 32$). Minima in detrital P concentrations correspond to intervals of high authigenic P contents (144 to 145.5 cm and 151 to 153.5 cm; Fig. 3). High amounts of Fe also characterize HLs, but as for detrital P, the statistical correlation with IRD is rather weak ($r^2 = 0.50$, $n = 32$). Fe ambient sedimentation levels are maintained, slightly increased, or even enhanced such as for 150.5- and 152-cm core depths at the bottom of HL 4 (Fig. 3). Finally, Fe concentrations follow the authigenic P concentration trend observed within HLs. In contrast with Holocene samples, in which Fe-bound P and Fe concentrations are closely linked (Fig. 2), HLs bear no signal of Fe-bound P (Fig. 3). The organic-bound P record is rather complex. Besides a downward decreasing trend in ambient (glacial and Holocene) sediments (Figs. 2 and 3), organic-bound P shows relative minima for HL 4 and less conspicuously for HL 5.

Molar TOC/P_{org} in ambient glacial sediments (193 ± 41; Fig. 5) provides values slightly higher than the Redfield ratio estimated for marine organic matter from nutrient data analysis (117 ± 14; Anderson and Sarmiento, 1994). In our samples, TOC/P_{org} generally displays lower values within HLs (148 ± 30). Oxygen and hydrogen contents of organic matter, represented by OI and HI indexes, display lower and higher values in HLs, respectively (Fig. 5). In an HI vs. OI plot, we observe two different sets of samples, corresponding to ambient glacial sediments and HL samples, respectively (Fig. 6a). The OI also covaries with organic matter $\delta^{13}C$ values: HL samples are characterized by low $\delta^{13}C$ values and OI, whereas ambient glacial sediments provide high $\delta^{13}C$ and OI (Fig. 6b).

In this study, only calcite, dolomite, and ankerite percentages from XRD are presented (Fig. 7). The occurrence of Heinrich events 4 and 5 is clearly brought into evidence: Calcite percentages show a twofold decrease compared to ambient glacial values, whereas dolomite and ankerite covary and increase during HL deposition (Fig. 7).

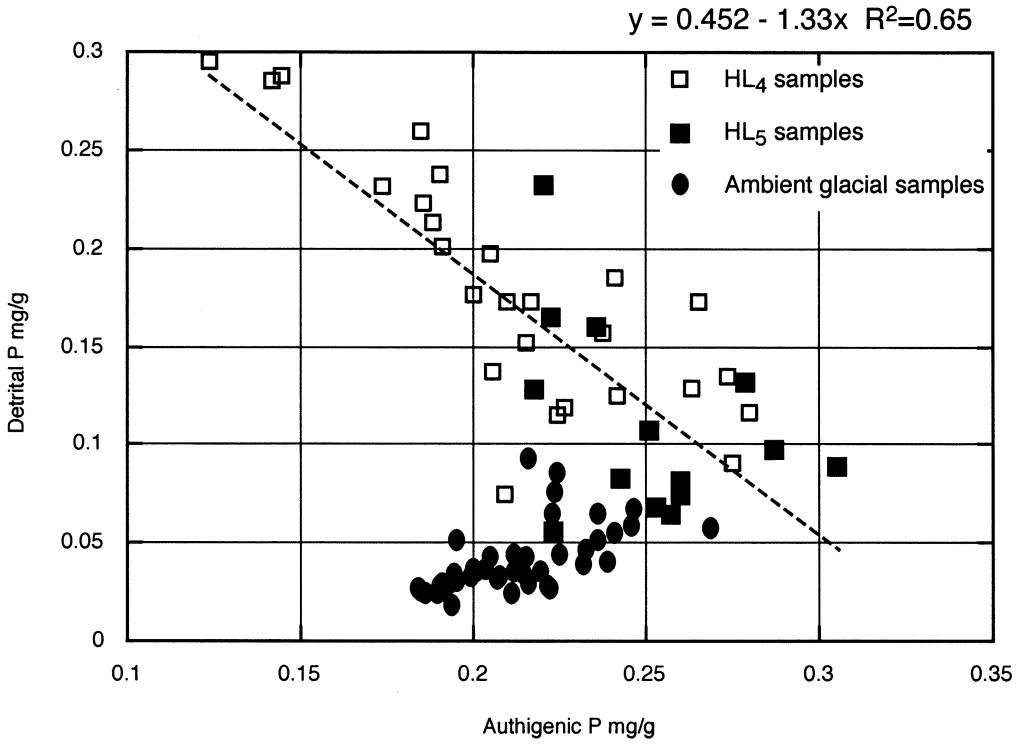

Fig. 4. Plot of authigenic P vs. detrital P concentrations for the <50-μm fraction of samples from core SU 90-09. Solid circles = ambient glacial sediment samples, empty squares = Heinrich layer (HL) 4 samples, solid squares = HL 5 samples. The regression line has been calculated using a least squares fit method (Beyer, 1976).

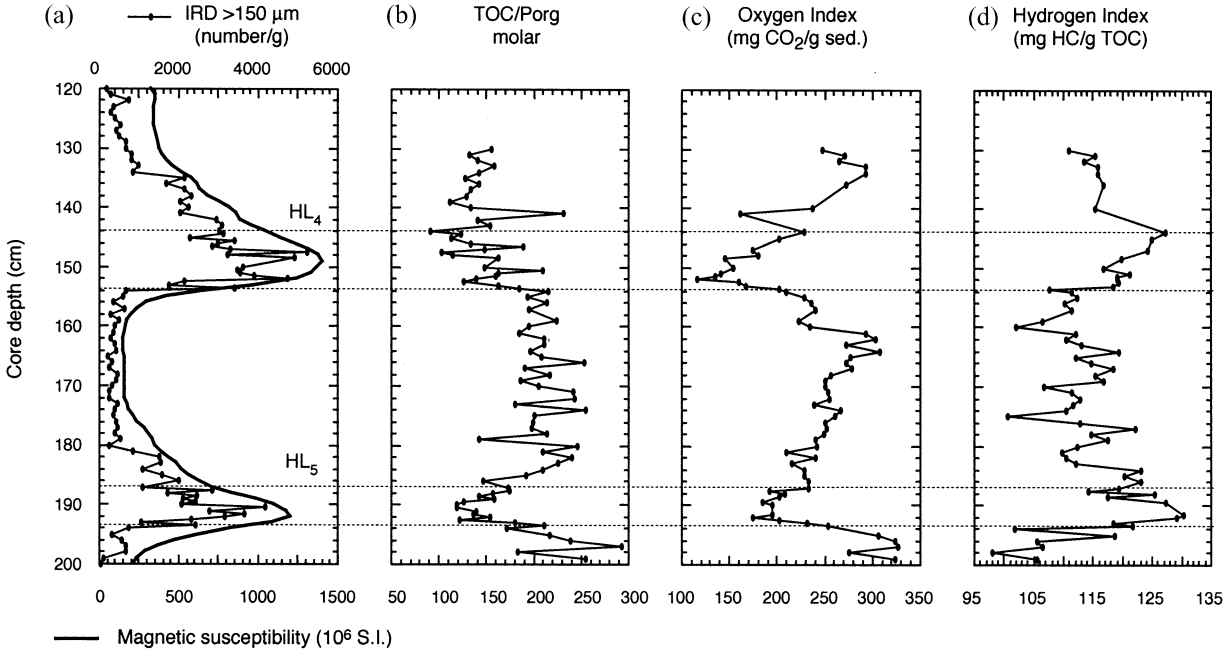

Fig. 5. Plots of down-core variations of (a) magnetic susceptibility and ice-rafted debris (IRD) (>150 μm) content (Grousset et al., 2001), (b) total organic carbon (TOC)/P of organic matter molar ratio (TOC values have been taken from Huon et al., 2002), (c) Rock-Eval oxygen index, and (d) Rock-Eval hydrogen index. HL = Heinrich layer.

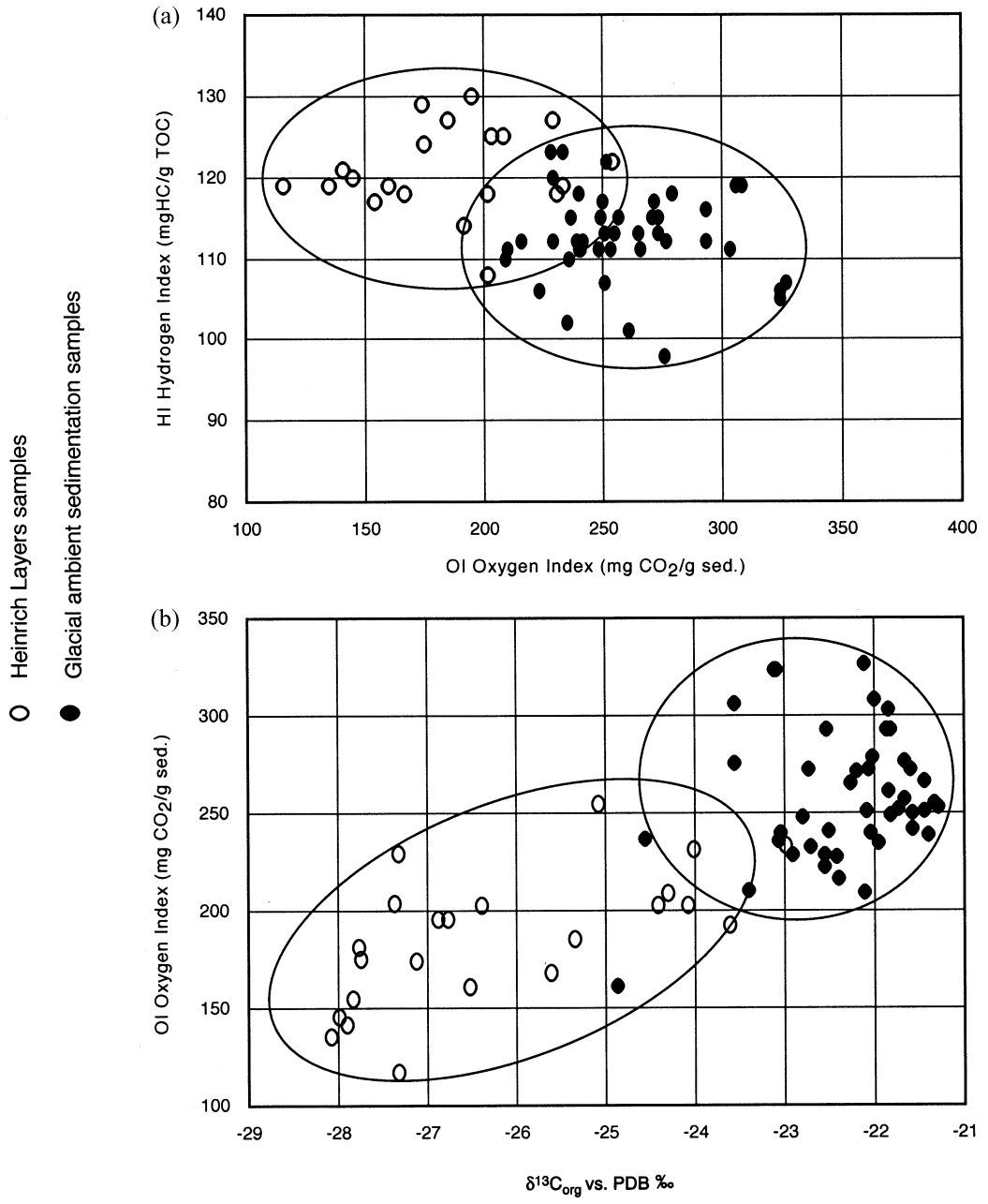

Fig. 6. (a) Plot of oxygen index (OI) vs. hydrogen index (HI) and (b) plot of $\delta^{13}C$ of organic carbon (Huon et al., 2002) vs. OI of fine-grained (<50-μm fraction) samples from core SU90-09. Solid symbols = ambient glacial sediment samples, empty symbols = Heinrich layers 4 and 5 samples. A clear, direct correlation between OI and $\delta^{13}C$ for Heinrich events samples appears. TOC = total organic carbon, sed. = sediment, PDB = Pee Dee Belemnite standard.

4. DISCUSSION AND INTERPRETATION

4.1. Evidence for the Lack of Major Postdeposition Diagenetic Redistribution of P

Since comparable values are obtained for Holocene and ambient glacial samples, it appears that no major late diagenetic process influenced the redistribution of authigenic and organic-bound P in sediments (Figs. 2 and 3). On the other hand, the higher Fe-bound P values displayed by Holocene sediments hint at a diagenetic imprint with respect to this phase. P adsorbed onto Fe oxyhydroxides minerals may easily be released into pore waters once Fe oxyhydroxides have been dissolved below the redox boundary (Jarvis et al., 1994). Thus, the observed differences between ambient glacial and Holocene samples may be the result of active adsorption-desorption processes taking place during the redox cycle in the upper section of the sediment column.

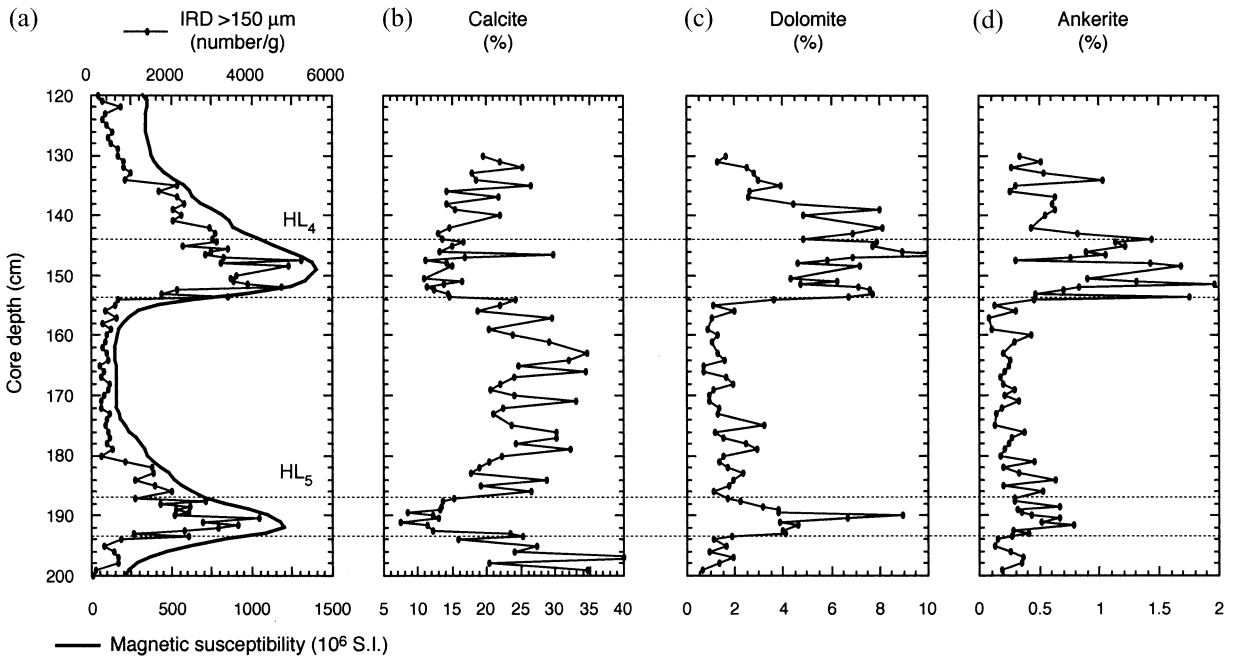

Fig. 7. Plots of down-core variations of (a) magnetic susceptibility and ice-rafted debris (IRD) (>150 μm) content (Grousset et al., 2001); (b) calcite, (c) dolomite, and (d) ankerite percentages of fine-grained (<50-μm fraction) sediments from core SU90-09.

4.2. Nature of the Authigenic P Phase

As discussed under "Material and Methods," the acetate step of the SEDEX method extracts phosphorus associated to different sedimentary phases (see above and Table 1). It is important here to determine which of these components are present in the studied sediments. Biogenic calcium carbonate does not generally bear large quantities of P ($<3.2 \times 10^{-6}$ mg/g; Sherwood et al., 1987; Delaney, 1998). In fact, phosphorus previously thought to be associated with carbonate shell debris, has been found to be principally bound to Fe-oxides coatings (Sherwood et al., 1987). For sediments from core SU 90-09, the correlation between the authigenic phosphorus phase and calcite is not significant ($r^2 = 0.083$), confirming that calcite is not a significant source of P to the sediments. Fish debris are an important component of sediments in upwelling margins and coastal areas, but in other environmental settings (e.g., deep sea), fish debris percentages are relatively low and mainly concentrated in the coarse fraction (Schenau et al., 2000). Phyllosilicates generally do not contain significant quantities of phosphorus (Ruttenberg, 1992), and in samples from core SU90-09, they average only 3% (XRD results, data not shown). However, we cannot exclude that a small part of the authigenic phosphorus is associated with phyllosilicates. Another possible component of this authigenic pool might be allochtonous authigenic phosphorus minerals, whose variations would not reflect active in situ precipitation. Because precipitation of authigenic P at the sediment-water interface is known to occur only in continental margin sediments below high-productivity zones (Froelich et al., 1988), a way to test for the presence of allochtonous material would be to know the concentration of the authigenic P phase in surface sediments. This value should give an indication of the amount of preformed authigenic P present in our sediments. On the basis of the data available to us, concentrations of authigenic phosphorus from below 10 cm and from ambient glacial samples are in the range of values previously reported for pelagic sediments (0.185 mg/g; Ruttenberg and Berner, 1993); this suggests the lack of an important contribution from an allochtonous source of authigenic phosphorus minerals. Sedimentary detrital apatite might also have been transported along with the ice-rafted material to site SU90-09. However, because phosphorus is generally tightly bound in the structure of sedimentary apatite, which is generally well crystallized (Compton et al., 2000), it would be more likely extracted during the third step of the SEDEX extraction.

The authigenic P concentration increases at the beginning and at the end of HL 4 and to a lesser extent within HL 5, possibly documenting (a) enhanced P release due to organic matter degradation, (b) increased input of nutrients (particulate and dissolved) supplied by ice rafting from the surrounding land masses, or (c) the northward penetration of nutrient-rich South Atlantic waters (Charles and Fairbanks, 1992). An argument against enhanced P regeneration from an organic matter source is that TOC/P_{org} decreases within HLs (Fig. 5), pointing to a relative enrichment of organic P with respect to organic carbon and possibly more refractory organic matter. The last two hypotheses can better account for the authigenic P behavior. In fact, higher nutrient levels during iceberg discharges, enhancing primary productivity, have already been suggested (Sancetta, 1992). However, we have no micropaleontological

evidence for such an increase, at least for core SU 90-09 (Grousset et al., 2001; Huon et al., 2002).

4.3. Enhanced Supply of Ice-Rafted Detrital P During Heinrich Events 4 and 5

Because detrital P is not involved in biologic processes (Delaney, 1998), its distribution can be regarded as mirroring detrital supply in sediments. The low point-to-point correlation between coarse IRD content and fine-grained detrital P in HLs may be explained by (a) the different behavior due to grain size and/or (b) the different source of detrital supply. Sr and Nd isotope analyses of IRD material indicate a succession and mixing of European and Canadian sources of detrital material for HL 4 (Grousset et al., 1993, 2000). Igneous and metamorphic rocks of these two geological provinces may possibly yield distinct amounts of P-bearing minerals (e.g., apatite, monazite), which could be reflected in detrital P sedimentary records. High amounts of detrital P are observed in the central interval of HL 4 (146 to 150.5 cm, Fig. 3), which is supposed to reflect enhanced supply from Canada (Grousset et al., 2000), while lower amounts of detrital P in the upper and bottom intervals of HL 4 could reflect a European origin (Fig. 3). Detrital P shows high values also within HL 5, but no sequential deposition could be detected, probably because this layer was deposited during a weaker ice-rafted discharge event (Bond et al., 1992), as is already shown by the low IRD content (Fig. 3).

In contrast to Holocene sediments, where a positive correlation exists (Fig. 2), Fe and Fe-bound P are decoupled within HLs 4 and 5 (Fig. 3). In fact, HLs bear no signal of Fe-bound P. This behavior can be related either to the nature of Fe phases or to changing environmental conditions (see discussion below). Accumulation of well-crystallized detrital iron-bearing minerals (e.g., hematite coated grains; see Bond and Lotti, 1995) probably took place during HL deposition. Since these minerals constitute a less efficient sink for dissolved P than, for instance, neoformed and amorphous Fe oxides (Slomp et al., 1996), Fe-bound P formation was limited. Moreover, if low-oxygen conditions developed in the upper sediments (see discussion below), reduced Fe would precipitate as Fe sulfides. Because amorphous Fe sulfides are also dissolved during the dithionite step of the SEDEX extraction (Slomp et al., 1996), the increase in the extracted Fe in HLs could indicate the presence of these minerals.

Ankerite and dolomite peaks coeval with Fe maxima have also been identified by XRD within HLs (Fig. 7). If dolomite and ankerite were supplied to the sediments only by detrital input, they should covary with calcite during HL deposition. The lack of covariation may point to a possible diagenetic origin of fine-sized dolomite and ankerite, although detrital input is not excluded. Indeed, idiomorphic crystals of dolomite have been observed within HL sediments (Jantschik, 1991). If neoformed by direct precipitation into the sediments, both carbonate minerals, especially ankerite, reflect reducing and oxygen-poor conditions in the sediments (Glenn et al., 1994; Malone et al., 1994), which are not favorable to Fe-bound P phase formation (Jarvis et al., 1994; Slomp et al., 1996). These aspects are addressed more precisely in the following section.

4.4. Bottom-Water Conditions During HL Deposition Inferred From P Phase Distribution

The inverse correlation between authigenic and detrital P concentrations inside HLs and the tight behavior of Fe-bound and detrital P throughout the sediments provide evidence of changing bottom-water conditions. We propose in fact that the relationships between authigenic and Fe-bound P and detrital P are not just the result of a dilution effect between the three phases but more likely reflect changing conditions in the sediments. This is particularly true for Fe-bound P. Reducible Fe increases during HL deposition (Fig. 3). If the conditions were ideal for the adsorption of phosphorus on Fe oxides, we would expect to see a concomitant increase of this phase, which is not the case (Fig. 3). Moreover, the lack of precipitation of Fe-bound P during HL deposition was not caused by the decrease of dissolved P in bottom and pore waters. Indeed, supply of material from the continent increased during the deposition of HLs, which possibly implies enhanced phosphorus input. Moreover, as inferred from Cd/Ca ratios, phosphorus concentrations in bottom waters were higher during Heinrich events (Bertram et al., 1995).

Fe-bound P and Authigenic apatite are precipitated in sediments only under specific chemical and physical conditions (e.g., relatively high oxygen content, low alkalinity, high fluoride pore-water content). Beyond these limiting conditions, dissolved P is released from the sediment back into the water column (Ingall and Jahnke, 1994; Jarvis et al., 1994). The adsorption of phosphate on Fe oxyhydroxides takes place in the oxidized layer and controls even on short-time scales the flux of phosphorus between marine sediments and bottom waters (Krom and Berner, 1980; Slomp and Van Raaphorst, 1993). Among the factors ruling this process, oxygen levels in pore waters and the availability and crystallinity of Fe oxyhydroxides are the most important (Anschutz et al., 1996; Slomp et al., 1996). Enhanced organic matter degradation, changes in productivity, and/or stratification of the water column may reduce oxygen levels in pore waters, hence making the oxidized layer thin or even absent. Under these conditions, Fe oxyhydroxides are dissolved, since Fe^{3+} is rapidly reduced to Fe^{2+}, leading to the precipitation of iron sulfides. Phosphate associated to the Fe oxides is then released to the pore waters and, if there are no Fe oxides available, to bottom waters. On the other hand, if the amount of iron is large enough to buffer for the precipitation of Fe sulfides, Fe oxyhydroxides may still be present and phosphates might be adsorbed, despite general reducing conditions (e.g., Mississippi delta sediments; Ruttenberg and Berner, 1993). The crystallinity of Fe oxyhydroxides also plays an important role because amorphous Fe oxide minerals (e.g., ferrihydrite) precipitate in situ, constitute a more efficient sink for phosphate than well-crystallized particles (e.g., goethite; Slomp et al., 1996). Thus, the presence vs. absence of the Fe-bound P phase, along with its relationship with Fe oxides, should give indications about both oxygen levels and the nature of the Fe particles.

It has been shown that massive discharge of icebergs during Heinrich events produced a freshwater lid, which possibly caused a temporary stratification of the water column, hampering or even shutting down NADW formation (Broecker, 1994; Sarnthein et al., 1994; Maslin et al., 1995; Vidal et al., 1997;

Chapman and Shackleton, 1999; Marchal et al., 1999). Low oxygen levels caused by reduced bottom-water ventilation may have led to dysaerobic conditions in the sediments. The disappearance of the oxidized layer may in turn have reduced authigenic P precipitation, promoted the precipitation of Fe sulfides, and inhibited adsorption of P on Fe particles (Berner and Rao, 1994; Jarvis et al., 1994). The concomitant drop of Fe-bound P and authigenic P concentrations within HLs may therefore indicate (a) the loss of dissolved P from the sediments to the water column, and/or (b) the reduced capability of HL sediments to retain phosphorus. Low oxygen levels, along with the different nature of Fe particles, may have completely inhibited the adsorption of phosphate, influencing pore-water and bottom-water phosphate concentration.

Because sediment accumulation rates increased during Heinrich events (Elliot et al., 1998; Grousset et al., 2001; Huon et al., 2002), the phosphorus concentrations may not reflect the amplitude of phosphorus supply to sediments. Using average sedimentation rates estimates of 3.4 and 10.3 cm ka^{-1}, average dry bulk sediment densities of 1.90 and 2.28 g cm^{-3}, and average fine-sized percentages of 30 and 39% for ambient glacial sediments and HLs, respectively (Huon et al., 2002), we have tried to estimate the theoretical release of P in the sediments during HL 4. We made the simple assumption that fine-sized Fe-bound P, lacking in HLs, should have precipitated in equal concentration as during ambient glacial sedimentation (average concentration $\pm 1\sigma$: 0.071 $\pm$ 0.0162 mg P g^{-1}). The phosphorus mass release rate (equivalent to the accumulation rate, P-MAR, mg P cm^{-2} ka^{-1}) is calculated using the following equation:

$$\text{P-MAR} = [\text{P}] \times F \times d \times S, \quad (1)$$

where d is the dry bulk sediment density (g cm^{-3}), S is the sedimentation rate (cm ka^{-1}), F is the fine-sized (<50 μm) fraction abundance (wt.%), and [P] is the fine-sized Fe-bound P concentration (mg P g^{-1}). The results of these calculations provide first-order estimates of 0.14 mg P cm^{-2} ka^{-1} during ambient glacial sedimentation and 0.65 mg P cm^{-2} ka^{-1} for HL 4. Approximately 4.6 more Fe-bound P should theoretically precipitate during HL 4. The overall amount of P released during Heinrich event 4 should be $\sim$1.24 mg P cm^{-2}, using an average duration of 1.9 ka (neighbor sediment core SU90-08; Vidal et al., 1997).

Additional estimates of P concentration release in the water column can be made using the following equation:

$$\text{P} = \text{P-MAR} \times (1/M_P) \times (1/H) \times (1/d), \quad (2)$$

where P is phosphorus concentration in bottom water (μmol P kg^{-1} seawater), P-MAR is the P mass accumulation rate previously calculated (mg P cm^{-2} ka^{-1}), M_P is P atomic mass (30.97 g mol^{-1}), H is the overlying seawater column possibly concerned by P release (estimated at 1315 m), and d is the seawater density (1.0253 g cm^{-3}). The parameter H has been calculated as the difference between the average depth of the Atlantic Ocean (3315 m) and a depth of 2000 m, at which increases in P and Cd concentrations have been reported (Bertram et al., 1995). Estimated concentrations of released P in bottom water are 0.16 μmol P kg^{-1} ka^{-1} or 0.30 μmol P kg^{-1} for 1.9 ka. We can compare this P concentration with previous estimations made using other proxies such as benthic foraminifer δ^{13}C and Cd/Ca ratios (Boyle, 1988; Bertram et al., 1995). An average δ^{13}C decrease of 0.35‰ was reported by Vidal et al. (1997) in the North Atlantic for benthic foraminifers in HLs 4 and 5. This offset possibly records an increase of Cd/Ca in the range 0.05 to 0.08 μmol mol^{-1} (data in Bertram et al., 1995) that can be converted in a bottom-water concentration of dissolved Cd of $\sim$0.25 nmol kg^{-1} (Boyle, 1988). Accordingly, the P concentration in bottom waters derived from the ΔCd-ΔP relation (Boyle, 1988; Bertram et al., 1995) increases by $\sim$1.2 μmol P kg^{-1} during Heinrich events. Although very imprecise because of numerous assumptions and uncertainties involved in the calculation, our result may explain $\sim$25% of the assumed phosphorus increase recorded during HL 4. With a higher estimation of sedimention rate in HLs (e.g., 15 cm ka^{-1}; Grousset et al., 2001), we can derive a higher P release (up to 0.23 μmol kg^{-1} ka^{-1}), but it will not drastically change our result (36%).

Because the phosphate adsorption/desorption cycle on Fe oxyhydroxides is restricted to the very top of the sediment column (Slomp et al., 1996), changes of this cycle may influence bottom-water properties on a very short time scale. Increased Cd/Ca ratios of benthic foraminifers during Heinrich events have been interpreted as evidence of deep phosphate- and nutrient-rich waters, probably from southern sources (e.g., Bertram et al., 1995). Although it is not possible here to assess the real impact of the release of dissolved P from the sediments, this process may have contributed to higher phosphate concentrations in bottom waters during Heinrich events. In this case, the Cd/Ca ratio could have recorded a local signal along with a remote source change.

4.5. Selective Preservation or Change in the Source of Organic Matter in HLs

During prominent Heinrich events (HLs 1 to 5), the relative contribution of terrestrial organic matter is clearly enhanced, as shown by carbon and nitrogen stable isotopic studies of the organic matter (Huon et al., 2002). Along with ambient marine organic matter, several continental sources have been postulated, including ancient soils from periglacial regions and organic matter–bearing rocks from the geological basement (e.g., carbonate rocks; Bond et al., 1992; Rosell-Melé et al., 1997).

Although TOC/P_{org} values measured in this study are close to the Redfield ratio of 117 $\pm$ 14 (Anderson and Sarmiento, 1994), they do not necessarily reflect a dominant marine signature in HLs with respect to the high values usually expected for continental sources (Ruttenberg and Gõni, 1997). Low values for continental organic matter can possibly reflect (a) a grain size effect (Ruttenberg and Goñi, 1997), also shown by the TOC/TN ratio (Keil et al., 1994; Huon et al., 2002); (b) the degree of organic matter mineralization in the source area; or (c) the selective preservation of organic matter in sediments.

HI and OI provide contrasting results for ambient glacial sediments and HLs. Low HI values are generally consistent with the signature of refractory organic matter (Espitalié et al., 1986), often observed in deep-sea environments (Zegouagh et al., 1999). Huon et al. (2002) interpreted the low δ^{13}C values in HLs as reflecting a dominant terrestrial origin for organic matter, including contributions from organic matter–bearing

rocks. The positive correlation between low OI and low $\delta^{13}C$ implies that continental organic matter deposited during Heinrich events has an oxygen-depleted composition (Fig. 6b). Thus, this relation is consistent with the hypothesis of a significant contribution of old and more refractory organic matter because it is known that during burial and maturation of the organic matter, the OI decreases (Hetenyi, 1998). The relatively low OI of HL samples, together with their somewhat higher HI, may also indicate that some of the organic matter has been better preserved from bacterial degradation during the phases of enhanced ice-rafting supply, in contrast to more intense oxidation during ambient glacial sedimentation. Higher sedimentation rates during HLs deposition also support this interpretation (Manighetti and McCave, 1995). In fact, during oxidation of organic matter, OI and HI are affected and show a trend toward higher and lower values, respectively (Meyers, 1997). This latter assumption is consistent with low-oxygen bottom-water conditions during Heinrich events shown by Fe-bound P and authigenic P depletions. On the whole, enhanced preservation due to high sedimentary fluxes as well as changing organic matter composition may explain both the observed OI and HI variations.

5. CONCLUSIONS

1. Using a sequential extraction of fine-grained (<50 μm) phosphorus phases (detrital, authigenic, Fe bound, and organic bound), we show that their down-core distribution in North Atlantic deep-sea sediments reflects rapidly changing environmental conditions. Millennial time scale episodes such as Heinrich events are recorded by changes in the distribution of sedimentary phosphorus phases.
2. During the phases of enhanced ice-rafting supply corresponding to HLs 4 and 5, dissolved P is lost from sediments because the conditions leading to Fe-bound P and authigenic P formation are no longer completely fulfilled. Stratification of the water column related to massive iceberg discharges account for these temporary suboxic-anoxic conditions in the sediments. Because fine-grained ankerite and dolomite may crystallize under the oxygen-depleted conditions prevailing during Heinrich events, their higher occurrences support this conclusion.
3. Detrital P, authigenic P, and Fe concentrations in HLs 4 and 5 reflect sequential depositions of ice-rafted detrital material that are closely tied to bottom-water oxic concentrations.
4. TOC vs organic-bound P ratios and Rock-Eval pyrolysis indices provide evidence for enhanced preservation of fine-grained sedimentary organic matter during Heinrich events, which is in line with less oxygenated bottom-water conditions and higher sedimentation rates. However, these parameters may also reflect the presence of more refractory and old organic matter originating from continental sources, as has been suggested by earlier C isotope studies (Huon et al., 2002), contrasting with the marine and terrigenous inputs prevailing during ambient glacial sedimentation of the past 50 ka.

Acknowledgments—The samples used in this study were taken from core SU90-09, recovered by R/V *Le Suroit* (IFREMER, France). The French CNRS program VARIENTE is acknowledged for providing all the samples. We are indebted to D. Burdloff, M. Lafosse, and R. Pouvreau (Département de Géologie et Océanographie, Université de Bordeaux I) for technical assistance. We gratefully aknowledge J. Ondrus and S. Pierrehumbert of the SCPE laboratory of the canton of Neuchâtel for inductively coupled plasma atomic emission spectroscopy. We thank T. E. Cerling, G. M. Filippelli, and an anonymous reviewer for their helpful suggestions.

Associate editor: T. E. Cerling

REFERENCES

Anderson L. A. and Sarmiento J. L. (1994) Redfield ratios of remineralization determined by nutrient data analysis. *Global Biogeochem Cycles* **8**, *1*, 65–80.

Anderson L. D. and Delaney M. L. (2000) Sequential extraction and analysis of phosphorus in marine sediments: Streamlining of the SEDEX procedure. *Limnol. Oceanogr* **42**, *2*, 509–515.

Andrews J. T. (1998) Abrupt changes (Heinrich events) in late Quaternary North Atlantic marine environments: A history and review of data and concepts. *J. Quat. Sci.* **13,** 3–16.

Anschutz P., Zhong S., Sundby B., Mucci A., and Gobeil C. (1996) Burial efficiency of phosphorus and the geochemistry of iron in continental margin sediments. *Limnol. Oceanogr.* **43,** 53–64.

Balesdent J. and Mariotti A. (1996) Measurement of soil organic matter turnover using ^{13}C natural abundance. In *Mass Spectrometry of Soils* (eds. T. W. Boutton and S.-I. Yamasaki), pp. 83–111. Marcel Dekker, New York.

Baturin G. N. (1988) Disseminated phosphorus in oceanic sediments—A review. *Mar. Geol.* **84,** 95–104.

Benson L. V., Burdett J. W., Kashgarian M., Lund S. P., Phillips F. M., and Rye R. O. (1996) Climatic and hydrological oscillations in the Owens lake basin and adjacent Sierra Nevada, California. *Science* **274,** 746–751.

Berner R. A. and Rao J.-L. (1994) Phosphorus in sediments of the Amazon river and estuary: Implications for the global flux of phosphorus to the sea. *Geochim. Cosmochim. Acta* **58,** 2333–2339.

Bertram C. J., Elderfield H., Shackleton N. J., and MacDonald J. A. (1995) Cadmium/calcium and carbon isotope reconstruction of the glacial northeast Atlantic Ocean. *Paleoceanography* **10**, *3*, 563–578.

Beyer W. H. (1976) *Standard Mathematical Tables*. CRC Press, Boca Raton, FL.

Bond G. C. and Lotti R. (1995) Icebergs discharges into the North Atlantic on millennial time scales during the last glaciation. *Science* **267,** 1005–1010.

Bond G. C., Heinrich H., Broecker W., Labeyrie L., McManus J., Andrews J., Huon S., Jantschik R., Clasen S., Simet C., Tedesco K., Kals M., Bonani G., and Ivy S. (1992) Evidence for massive discharges of icebergs into the North Atlantic ocean during the last glacial period. *Nature* **360,** 245–249.

Bond G. C., Broecker W., Johnsen S., McManus J., Labeyrie L., Jouzel J., and Bonani G. (1993) Correlations between climate records from North Atlantic sediments and Greenland ice. *Nature* **365,** 143–147.

Boyle E. A. (1988) Cadmium: Chemical tracer of deep-water paleoceanography. *Paleoceanography* **3,** 471–489.

Broecker W. S. (1994) Massive iceberg discharges as triggers for global change. *Nature* **372,** 421–424.

Broecker W. S., Bond G. C., Klas M., Clark E., and McManus J. (1992) Origin of the Northern Atlantic's Heinrich events. *Clim. Dyn.* **6,** 265–273.

Chapman M. R. and Shackleton N. J. (1999) Global ice-volume fluctuations, North Atlantic ice-rafting events, and deep-ocean circulation changes between 130 and 70 ka. *Geology* **27**, *9*, 795–798.

Charles C. D. and Fairbanks R. G. (1992) Evidence from Southern Ocean sediments for the effect of North Atlantic deep-water flux on climate. *Nature* **355,** 416–419.

Christensen B. T. (1996) Physical fractionation of soil and organic matter in primary particle size and density separates. In *Advances in Soil Science, Vol. 20* (ed. B. A. Steward), pp. 1–76. Springer-Verlag, New York.

Colman A. S. and Holland H. D. (2000) The global diagenetic flux of phosphorus from marine sediments to the oceans: Redox sensitivity

and the control of atmospheric oxygen levels. *Marine Authigenesis: From Global to Microbial, Vol. 66*, pp. 53–75. Society for Sedimentary Geology, Tulsa, OK.

Compton J., Mallison D., Glenn C. R., Filippelli G., Föllmi K., Shields G., and Zanin Y. (2000) Variations in the global phosphorus cycle. In *Marine Authigenesis: From Global to Microbial, Vol. 66*, (eds. C. R. Glenn, L. Prevot-Lucas, and J. Lucas) pp. 21–33. Society for Sedimentary Geology, Tulsa, OK.

Cortijo E., Yiou P., Labeyrie L., and Cremer M. (1995) Sedimentary record of rapid climatic variability in the North Atlantic Ocean during the last glacial cycle. *Paleoceanography* **10,** 911–926.

Delaney M. L. (1998) Phosphorus accumulation in marine sediments and the oceanic phosphorus cycle. *Global Biogeochem. Cycles* **12**,*4*, 563–572.

Eaton A. D., Clesceri L. S., and Greenberg A. E. (1995) *Standard Methods for the Examination of Water and Wastewater*. 19th ed. American Public Health Association, Washington, DC.

Elliot M., Labeyrie L., Bond G. C., Cortijo E., Turon J-L., Tisnerat N., and Duplessy J. C. (1998) Millennial-scale iceberg discharges in the Irminger Basin during the last glacial period: Relationship with the Heinrich events and environmental settings. *Paleoceanography* **13**, *5*, 433–446.

Espitalié J., Deroo G., and Marquis F. (1986) La pyrolyse Rock-Eval et ses applications—III partie. *Rev. Inst. Fr. Pet.* **41**, *1*, 73–89.

Filippelli G. M. and Delaney M. L. (1996) Phosphorus geochemistry of equatorial Pacific sediments. *Geochim. Cosmochim. Acta* **60,** 1479–1495.

Föllmi K. B. (1996) The phosphorus cycle, phosphogenesis and marine phosphate-rich deposits. *Earth Sci. Rev.* **40,** 55–124.

Froelich P. N., Arthur M. A., Burnett W. C., Deakin M., Hensley V., Jahnke R., Kaul L., Kim K. H., Roe K., Soutar A., and Vathakanon C. (1988) Early diagenesis of organic matter in Peru continental margin sediments; phosphorite precipitation. The origin of marine phosphorite; the results of the R.V. Robert D. Conrad cruise 23-06 to the Peru shelf. *Mar. Geol.* **80**, *3-4*, 309–343.

Glenn C. G., Föllmi K. B., Riggs S. R., Baturin G. N., Grimm K. A., Trappe J., Abed A. M., Galli-Olivier C., Garrison R. E., Ilyin A. V., Jehl C., Rohrlich V., Sadaqah R. M. Y., Schidlowski M., Sheldon R. E., and Siegmund H. (1994) Phosphorus and phosphorites: Sedimentology and environments of formation. *Eclogae Geol. Helv.* **87**, *3*, 747–788.

Grimm E. C., Jacobson G. L., Watts W. A., Hansen B. C. S., and Maasche K. A. (1993) A 50,000-year record of climate oscillations from Florida and its temporal correlation with the Heinrich events. *Science* **261,** 198–200.

Grousset F. E., Labeyrie L., Sinko J. A., Cremer M., Bond G. C., Duprat J., Cortijo E., and Huon S. (1993) Patterns of ice-rafted detritus in the glacial North Atlantic. *Paleoceanography* **8**, *2*, 175–192.

Grousset F. E., Pujol C., Labeyrie L., Auffret G., and Boelaert A. (2000) Were the North Atlantic Heinrich events triggered by the behavior of the European ice sheets. *Geology* **28**, *2*, 123–126.

Grousset F. E., Cortijo E., Huon S., Hervé L., Richter T., Burdloff D., Duprat J., and Weber O. (2001) Zooming in on Heinrich layers. *Paleoceanography* **16,** 240–259.

Heinrich H. (1988) Origin and consequences of cyclic ice rafting in the Northeast Atlantic Ocean during the past 130,000 years. *Quat. Res.* **29,** 142–152.

Hetenyi M. (1998) Oxygen index as an indicator of early organic maturity. *Org. Geochem.* **29**, *1-3*, 63–77.

Huon S. and Ruch P. (1992) Mineralogical, K-Ar and $^{87}Sr/^{86}Sr$ isotope studies of Holocene and Late Glacial sediments in a deep core from the northeast Atlantic Ocean. *Mar. Geol.* **107,** 275–282.

Huon S. and Jantschik R. (1993) Detrital silicates in Northeast Atlantic deep-sea sediments during the Late Quaternary: Major elements, REE and Rb-Sr isotopic data. *Eclogae Geol. Helv.* **86**, *1*, 195–218.

Huon S., Grousset F. E., Burdloff D., Bardoux G., and Mariotti A. (2002) Sources of fine-sized organic matter in North Atlantic Heinrich Layers: $\delta^{13}C$ and $\delta^{15}N$ tracers. *Geochim. Cosmochim. Acta* **66,** 223–239.

Ingall E. and Jahnke R. (1994) Evidence for enhanced phosphorus regeneration from marine sediments overlain by oxygen depleted waters. *Geochim. Cosmochim. Acta* **58,** 2571–275.

Jantschik R. (1991) Mineralogische und Geochemische Untersuchungen Spätquartärer Tiefseesedimente aus dem Westeuropäischen Becken. (bei 47°30' N und 19°30' W). Ph.D. thesis, University of Neuchâtel.

Jantschik R. and Huon S. (1992) Detrital silicates in northeast Atlantic deep-sea sediments during the late Quaternary: Mineralogical and K-Ar data. *Eclogae Geol. Helv.* **85,** 195–212.

Jarvis I., Burnett W. C., Nathan Y., Almbaydin F. S. M., Attia A. K. M., Castro L. N., Flicoteaux R., Hilmy M. E., Husain V., Qutawnah A. A., Serjani A., and Zanin Y. N. (1994) Phosphorite geochemistry: State-of-art and environmental concerns. *Eclogae Geol. Helv.* **87**, *3*, 643–700.

Keil R. G., Tsamakis E., Fuh C. B., Giddins J. C., and Hedges J. I. (1994) Mineralogical and textural controls on the organic composition of coastal marine sediments: Hydrodynamic separation using SPITT-fractionation. *Geochim. Cosmochim. Acta* **58,** 879–893.

Krajewski K. P., Van Cappellen P., Trichet J., Kuhn O., Lucas J., Martin-Algarra A.,, Prévot L., Tewari V. C., Gaspar L., Knight R. I., and Lamboy M. (1994) Biological processes and apatite formation in sedimentary environments. *Eclogae Geol. Helv.* **87**, *3*, 701–745.

Krom M. D. and Berner R. A. (1980) Adsorption of phosphate in anoxic marine sediments. *Limnol. Oceanogr* **25**, *5*, 797–806.

Kübler B. (1987) *Dosage Quantitatif des Minéraux Majeurs des Roches Sédimentaires par Diffraction X*. Cahier de l'Institut de Géologie de Neuchâtel Série ADX.

Kübler B., Jantschik R., and Huon S. (1990) Minéralogie et granulométrie des poussières éoliennes, dites "saharienne," du 24 avril 1989 à Neuchâtel. Leur importance pour l'environment, les sols et les sédiments. *Bulletin de la Société Neuchateloise des Sciences Naturelles* **113,** 75–98.

Lowell T. V., Heusser C. J., Andersen B. G., Moreno P. I., Hauser A., Heusser L. E., Schlüchter C., Marchant D. R., and Denton G. H. (1995) Interhemispheric correlation of Late Pleistocene glacial events. *Science* **269,** 1541–1549.

Malone M. J., Baker P. A., and Burns S. J. (1994) Recrystallization of dolomite; evidence from the Monterey Formation (Miocene), California. *Sedimentology* **41**, *6*, 1223–1239.

Mangerud J., Andersen S. T., Berglund B. E., and Donner J. J. (1974) Quaternary stratigraphy of Nordern: A proposal for terminology and classification. *Boreas* **3,** 109–128.

Manighetti B. and McCave I. N. (1995) Depositional fluxes, paleoproductivity, and ice rafting in the NE Atlantic over the past 30 ka. *Paleoceanography* **10**, *3*, 579–592.

Marchal O., Stocker T. F., and Joos F. (1999) Physical and biogeochemical responses to freshwater-induced thermohaline variability in a zonally averaged ocean model. In *Mechanisms of Global Climate Change at Millennial Time Scales, Vol. 112* (eds. P. U. Clark, R. S. Webb, and L. D. Keigwin), pp. 263–284. American Geophysical Union, Washington, DC.

Maslin M. A., Shackleton N. J., and Pflaumann U. (1995) Surface water temperature, salinity, and density changes in the northeast Atlantic during the last 45,000 years: Heinrich events, deep water formation, and climatic rebounds. *Paleoceanography* **10**, *3*, 527–544.

Meyers P. S. (1997) Organic geochemical proxies of paleoceanographic, paleolimnologic, and paleoclimatic processes. *Org. Geochem.* **27**, *5-6*, 213–250.

Paillard D. and Labeyrie L. D. (1994) Role of the thernohaline circulation in the abrupt warming after Heinrich events. *Nature* **372,** 162–164.

Rosell-Melé A., Maslin M. A., Maxwell J. R., and Schaeffer P. (1997) Biomarker evidence for "Heinrich" events. *Geochim. Cosmochim. Acta* **61,** 1671–1678.

Ruddiman W. F. (1977) Late Quaternary deposition of ice-rafted sand in the subpolar North Atlantic (lat. 40° to 65°N). *Geol. Soc. Am. Bull.* **88,** 1813–1827.

Ruttenberg K. C. (1992) Development of a sequential extraction method for different forms of phosphorus in marine sediments. *Limnol. Oceanogr.* **37**, *7*, 1460–1482.

Ruttenberg K. C. and Berner R. A. (1993) Authigenic apatite formation and burial in sediments from non-upwelling, continental margin environments. *Geochim. Cosmochim. Acta* **57,** 991–1007.

Ruttenberg K. C. and Gõni M. A. (1997) Phosphorus distribution, C:N:P ratios, and $\delta^{13}C_{oc}$ in artic, temperate, and tropical coastal sed-

iments: Tools for characterizing bulk sedimentary organic matter. *Mar. Geol.* **139,** 123–145.

Sancetta C. (1992) Primary productivity in the glacial North Atlantic and North Pacific oceans. *Nature* **360,** 249–251.

Sanchez-Gõni M. F., Turon J.-L., Eynaud F., and Gendreau S. (2000) European climatic response to millennial-scale changes in the atmosphere-ocean system during the Last Glacial period. *Quat. Res.* **54,** 394–403.

Sarnthein M., Winn K., Jung S., Duplessy J. C., Labeyrie L., Erlenkeuser H., and Ganssen G. (1994) Changes in East Atlantic deep-water circulation over the last 30,000 years—An eight time slice reconstruction. *Paleoceanography* **9,** 209–268.

Schenau S. J., Slomp C. P., and De Lange G. J. (2000) Phosphogenesis and active phosphorite formation in sediments from the Arabian Sea oxygen minimum zone. *Mar. Geol.* **169**, *1-2*, 1–20.

Schulz H., von Rad U., and Erklenkeuser H. (1998) Correlation between Arabian Sea and Greenland climate oscillations of the past 110,000 years. *Nature* **393,** 54–57.

Scintag. (1987) *PAD V, Diffraction System, Users Manual*. Scintag.

Sherwood B. A., Sager S. L., and Holland H. D. (1987) Phosphorus in foraminiferal sediments from North Atlantic Ridge cores and in pure limestones. *Geochim. Cosmochim. Acta* **51,** 1861–1886.

Slomp C. P. (1997) *Early Diagenesis of Phosphorus in Continental Margin Sediments*. Ph.D. thesis. Instituot voor Onderzoek der Zee, Den Burg, Texel, The Netherlands.

Slomp C. P. and Van Raaphorst W. (1993) Phosphate adsorption in oxidized marine sediments. *Chem. Geol.* **107,** 477–480.

Slomp C. P., Van der Gaast S. J., and Van Raaphorst W. (1996) Phosphorus binding by poorly crystalline iron oxides in North Sea sediments. *Mar. Chem.* **52,** 55–73.

Tyrrell T. (1999) The relative influences of nitrogen and phosphorus on oceanic primary production. *Nature* **400,** 525–531.

Van Cappellen P. and Ingall E. D. (1994) Benthic phosphorus regeneration, net primary production, and ocean anoxia: A model of the coupled marine biogeochemical cycles and phosphorus. *Paleoceanography* **9**, *5*, 677–698.

Vidal L., Labeyrie L. D., Cortijo E., Arnold M., Duplessy J. C., Michel E., Becque S., and Van Weering T. C. E. (1997) Evidence for changes in the North Atlantic deep water linked to meltwater surges during the Heinrich events. *Earth Planet. Sci. Lett.* **146,** 13–27.

Wang L., Sarnthein M., Erlenkeuser H., Grimalt J., Grootes P., Heilig S., Ivanova E., Kienast M., and Pflaumann U. (1999) East Asian Monsoon climate during the Late Pleistocene: High-resolution sediment records from the South China Sea. *Mar. Geol.* **156,** 245–284.

Zahn R., Schönfeld J., Kudrass H. R., Park M. H., Erlenkeuser H., and Grootes P. (1997) Thermohaline instability in the North Atlantic during meltwater events: Stable isotope and ice-rafted detritus records from core SO75 26KL, Portuguese margin. *Paleoceanography* **12**, *5,* 696–710.

Zegouagh Y., Derenne S., Largeau C., Bertrand P., Sicre M.-A., Saliot A., and Rousseau B. (1999) Refractory organic matter in sediments from the north-west African upwelling system: Abundance, chemical structure and origin. *Org. Geochem.* **30,** 101–117.